Anchoring non-antimicrobial molecules into mesoporous silica particles improves their antimicrobial power

María Ruiz-Rico[a*], Édgar Pérez-Esteve[a], Cristina de la Torre[b,c], Ana I. Jiménez-Belenguer[d], Amparo Quiles[e], María D. Marcos[b,c], Ramón Martínez-Máñez[b,c], José M. Barat[a]

[a] Grupo de Investigación e Innovación Alimentaria. Departamento de Tecnología de Alimentos, Universitat Politècnica de València. Camino de Vera s/n, 46022, Valencia, Spain

[b] Instituto Interuniversitario de Investigación de Reconocimiento Molecular y Desarrollo Tecnológico (IDM), Unidad Mixta Universitat Politècnica de València – Universitat de València. Departamento de Química, Universitat Politècnica de València, Camino de Vera s/n, 46022, Valencia, Spain

[c] CIBER de Bioingeniería, Biomateriales y Nanomedicina (CIBER-BBN)

[d] Departamento de Biotecnología, Universitat Politècnica de València. Camino de Vera s/n, 46022, Valencia, Spain

[e] Grupo de Microestructura y Química de Alimentos. Departamento de Tecnología de Alimentos, Universitat Politècnica de València. Camino de Vera s/n, 46022, Valencia, Spain

*Corresponding author: Phone: +34 963877000 ext. 83612; E-mail address: edpees@upv.es (E. Pérez-Esteve).

Abstract

Developing new antimicrobials and food preservative agents with innovative modes of action is an urgent task to fight against the escalating growth of resistant bacterial strains. In this scenario, nanotechnology has an important role to play due to, among others, their high surface per volume ratio.In the present study the capability of silica nanoparticles to anchor and concentrate the content of a non-antimicrobial considered molecule is demonstrated. With this aim, polyamines have being covalently linked to the external surface of MCM-41 nanoparticles. The developed organic-inorganic hybrid system was tested according to its antimicrobial activity. Results showed that the surface concentration of amines on the surface of the nanoparticles is so effective that immobilized-amines were 100 times more effective in killing *Listeria monocytogenes* bacteria than the same amount of free polyamines. This novel approach for the creation of antimicrobial nanodevices opens the possibility to put in value the antimicrobial power of natural molecules that have been discarded because of its low antimicrobial power.

Keywords: amine corona; bactericidal activity; *Listeria monocytogenes*; mesoporous silica nanoparticles; surface functionalization

1. Introduction

Bacterial infection is one of the most serious risks in the development of foodborne illnesses. To fight against pathogen and alterative microflora, an indiscriminate use of pesticides, food preservatives and antibiotics have been used in recent years, yielding as a consequence the apparition of a growing number of resistant strains.[1] In this context, the development of novel antibacterial systems as an alternative to classical antibiotics is an urgent need. For that, nanotechnology, defined as the manipulation of matter at an atomic and molecular level, is viewed as an excellent opportunity to achieve it.

Ones of the most explored nanostructured systems in the search of new antimicrobial systems are mesoporous silica nanoparticles (MSNs). MSNs are characterized by exhibiting a high stability, large specific surface area and volume, controllable size, easy surface functionalization, high biocompatibility and poorer hemolytic activity than their non-porous counterparts.[2-8] Due to these properties, some authors have reported the use of loaded and/or functionalized MSNs as antibacterial agents. Molina-Manso et al. used SBA-15 to encapsulate three different antimicrobial agents: vancomycin, rifampicin and linezolid.[9] Park and coauthors (2012) encapsulated allyl isothiocyanate in a mesoporous silica particle reaching a bacteria growth management.[10] Bernardos et al. used MCM-41 to encapsulate essential oils, achieving an important growth reduction of *Aspergillus niger* in comparison with non-encapsulated essential oils.[11] More recently, Yu and coauthors described the use of poly(*N*-isopropylacrylamide)-gated Fe_3O_4-MSNs core shell nanoparticles for the temperature-triggered release of antibacterial enzyme lysozyme,[12] and we stated the antimicrobial effect of caprylic acid incorporated in MSNs.[13]

Following an alternative approach, Li and Wang reported the use of lysozyme-coated MSNs as antibacterial agents,[14] and Qi et al. used vancomycin-modified MSNs to kill pathogenic gram-positive bacteria.[15] The same year, some of us reported the use of MCM-41 nanoparticles capped with ε-poly-l-lysine with high antibacterial activity against Gram-negative bacteria demonstrating

the possibility of improving the antimicrobial effect of a molecule by functionalization on the surface of a suitable support.[16]

Delving into this line, the goal of this work was to evaluate the effect of the concentration of a non-considered antimicrobial molecule through the anchoring into the surface of a MSN on their antimicrobial activity against one of the most distributed food-borne pathogen; i.e. *Listeria monocytogenes*.

2. Materials and methods

2.1. Chemicals

Tetraethylorthosilicate (TEOS), *N*-cetyltrimethylammonium bromide (CTABr), NaOH, *N*-(3-trimethoxysilylpropyl)diethylenetriamine (N3) and diethylenetriamine were provided by Sigma (Sigma-Aldrich, Madrid, Spain). *N*-[3-(trimethoxysilyl)propyl]ethylenediamine triacetic acid trisodium salt (C3) was provided by Fluorochem (Hadfield, UK).

2.2. Mesoporous silica nanoparticles synthesis

MCM-41 nanoparticles were synthesized by the procedure described by Ruiz-Rico et al.[13] The molar ratio of the reagents was fixed at 1 TEOS:0.1 CTABr:0.27 NaOH:1000 H_2O. NaOH was added to the CTABr solution, and the solution temperature was adjusted to 95 ºC. TEOS was then added dropwise to the surfactant solution. The mixture was allowed to stir for 3 h and yield a white precipitate. After synthesis, the solid was recovered by centrifugation, washed with distilled water, and air-dried at room temperature. The as-synthesized solid was calcined at 550 ºC in an oxidant atmosphere for 5 h to remove the template phase.

2.3. Functionalization of mesoporous silica nanoparticles

The surfaces of bare MSNs were functionalized with *N*-(3-trimethoxysilylpropyl)diethylenetriamine (N3) or with *N*-[3-(trimethoxysilyl)propyl]ethylenediamine triacetic acid trisodium salt (C3) following a similar procedure to that described by Pérez-Esteve et al.[17] To obtain amine-functionalized particles (**N3-N**), 1 g of MSNs was suspended in 40 mL of acetonitrile, and excess N3 (4.3 mL, 15.0 mmol/g) was added. To obtain carboxylate-functionalized particles (**C3-N**), 1 g of MSNs was suspended in 30 mL of water, and excess C3 (5.5 mL, 15.0 mmol/g) was added. Final mixtures were stirred for 5.5 h at room temperature. Finally, solids were filtered, washed with 30 mL of distilled water and dried at room temperature.

2.4. Materials characterization

Synthesized materials were characterized by standard techniques: transmission electron microscopy (TEM), field emission scanning electron microscopy (FESEM), particle size distribution, zeta potential and thermogravimetric analysis. TEM images were taken by a Philips CM10 (Philips electronics, Eindhoven, The Netherlands), which operated at an acceleration voltage of 80 kV. FESEM images were acquired with a Zeiss Ultra 55 (Carl Zeiss NTS GmbH, Oberkochen, Germany) and observed in the secondary electron mode. The particle size distribution of the different MSNs was determined by Zetasizer Nano ZS instrument (Malvern Instruments, UK). For measurements, solids were dispersed in Ringer buffer (RB) (0.22% NaCl, 0.011% KCl, 0.012% $CaCl_2$ and 0.005% $NaHCO_3$ in distilled water). All the measurements were taken in triplicate on previously sonicated highly dilute dispersions. To determine the zeta potential of the bare and functionalized MSNs, a Zetasizer Nano ZS (Malvern Instruments, UK) was used. Samples were dispersed in RB at the 1 mg/mL concentration and were sonicated for 2 min to preclude aggregation. The zeta potential was calculated from the particle mobility values by applying the Smoluchowski model. The average of five recordings was reported as the zeta potential. The degree

of functionalization of the different particles was determined by thermogravimetric analyses. Determinations were made on a TGA/SDTA 851e Mettler Toledo balance (Mettler Toledo Inc., Schwarzenbach, Switzerland), with a heating program that consisted in a heating ramp of 10° per minute from 273 to 373 K followed by an isothermal heating step at this temperature for 60 min in a nitrogen atmosphere (80 mL/min). Then, the program was allowed to continue with a dynamic heating segment from 373 to 1273 K in an oxidant atmosphere (air, 80 mL/min) and with an isothermal heating step at this temperature for 30 min.

2.5. Microbiological assays

Plate Count Agar (PCA) and Tryptic Soy Broth (TSB) were used to grow bacteria and to prepare inoculums. TSB and RB were used in the bacterial viability assays. Selective medium, Palcam Agar supplemented with polymyxin B, acriflavine was used to grow the treated *Listeria monocytogenes*. All the media were provided by Scharlau (Barcelona, Spain).

L. monocytogenes (CECT 936) was obtained from the Colección Española de Cultivos Tipo (CECT; Valencia, Spain). Bacterial stocks were stored at 4 ºC in PCA before use. Bacterial cells were grown aerobically in TSB at 37 ºC for 24 h to obtain a cell concentration of approximately 1 x 10^8 cells/mL. For the assays in RB, the inoculum was centrifuged at 4,000 rpm for 5 min and the obtained bacteria pellet was resuspended in the buffer.

2.6. Viability assessment

The study of the influence of bare and functionalized MSNs on the viability of *L. monocytogenes* was tested within a range of concentrations between 0 and 0.15 mg of solid per mL of Ringer buffer. In parallel, the influence of free amines (diethylenetriamine) was tested with a range of concentrations, which arranged from 0 to 3 mg/mL. Ringer buffer was used to ensure that the

surface charge of particles was not influenced by the components of the solvent. All the treatments were set in triplicate. Positive and negative controls were included in all the assays.

Particle stock suspensions were prepared in RB and were sonicated in 3 cycles of 5 minutes to facilitate the suspension and preclude agglomerates. To achieve the final concentrations of particles, different volumes of particle suspension were added to 30 mL of RB in Erlenmeyer flasks. Finally, flasks were inoculated with 100 µL (*L. monocytogenes*) of washed inoculum, to provide a cell density of approximately 10^5 CFU/mL, and were incubated under orbital stirring (150 rpm) at 37 ºC. Bacterial viability was quantified by preparing serial dilutions of the incubation mixtures and plating them on selective agar at 2 h of incubation. Plates were incubated at 37 ºC for 24-48 h, and then the CFUs per milliliter were determined. These values were logarithmically transformed and expressed as log CFU/mL. The control positive values were used to quantify growth of microorganisms and to calculate the survival percentage of bacteria.

2.7. Detection of morphological changes in bacterial cells

To study the morphological changes in *L. monocytogenes* cells caused by MSNs treatment, TEM observations were made. The cells treated with bare and functionalized MSNs, were collected at the end of the treatment by vacuum filtration (0.45 µm) under sterile conditions. Pellets were collected and fixed with 25 g/L glutaraldehyde solution for 24 h at 4 ºC and were post-fixed with 20 g/L osmium tetroxide solution for 1.5 h. Cells were centrifuged and the pellet was collected after each process step.

After this process, cells were stabilized by mixing them with a low gelling temperature agarose solution (3%, p/v) at 30 ºC, which facilitates fixation and embedding prior to TEM observation.[18] Next the cells inserted in the solidified agar were cut into cubes (1 mm^3). These cubes were fixed with 25 g/L glutaraldehyde solution, post-fixed with 20 g/L osmium tetroxidesolution, dehydrated with 30 g/L, 50 g/L, 70 g/L ethanol and 100 g/L, contrasted with uranyl acetate solution (20 g/L)

and embedded in epoxy resin (Durcupan, Sigma–Aldrich, St. Louis, MO, USA). The obtained blocks were cut by a Reichter-Jung ULTRACUT ultramicrotome (Leica Mycrosystems, Wetzlar, Germany). The obtained ultrathin sections (0.1 µm) were collected in copper grids and stained with 20 g/L acetate uranile and 40 g/L lead citrate to be observed in a JEOL JEM 2100F (JEOL Europe SAS, Croissy-sur-Seine, France) at 200 kV.

2.8. Determination of bacterial viability and agglomeration by fluorescence assay

A two-color fluorescent assay, LIVE/DEAD® BacLightTM (Life Technologies, Gaithersburg, MD, USA), was used to visualize viable and dead *L. monocytogenes* cells.[19] The kit provides a two-color assay of bacterial viability. SYTO 9 (green-fluorescent nucleic acid stain) labels all bacteria, with either intact or damaged membranes. In contrast, propidium iodide (red-fluorescent nucleic acid stain) penetrates only the bacteria with damaged membranes, which causes a reduction in SYTO 9 stain fluorescence when both dyes are present.

The two provided dye components were mixed at a 1:1 ratio. Next 0.8 µL of SYTO 9/propidium iodide were added to 500 µL of the treated suspension, and were mixed and incubated for 10 min to facilitate the penetration of dyes. Then, 5 µL of stained bacteria were applied to poly-L-lysine-covered slides for immunofluorescence (Sigma-Aldrich, Madrid, Spain), and a coverslip was placed over the suspension and sealed. The preparation was incubated for 5-10 min at room temperature in the dark to allow bacteria to adhere to slides. Slides were then observed under an Olympus BX50 fluorescence microscope equipped with an Olympus DP71 camera and a BA515IF barrier filter.

2.9. WST-1 Cell viability assays

For the cell culture experiments, trypan blue solution (0.4%) cell culture grade and dimethyl sulfoxide (DMSO), phosphate buffered saline (PBS) and Dulbecco's Modified Eagle's medium

(DMEM) with glucose, L-glutamine and pyruvate for cell culture were provided by Sigma-Aldrich (Poole, Dorset, UK). Mc Coy's 5a Medium and Keratinocyte Serum Free Medium, Fetal Bovine Serum (FBS) and trypsin were purchased from Gibco (Life Technologies, Madrid, Spain). Cell proliferation reagent WST-1 was purchased from Roche Applied Science (Barcelona, Spain).

HeLa human cervix adenocarcinoma and HEPG2 human liver carcinoma were grown in DMEM supplemented with 10% FBS. HCT116 human colon carcinoma cells were grown in McCoy's 5a Medium Modified supplemented with 10% FBS, HK2 homo sapiens kidney papilloma cells were grown in Keratinocyte Serum Free Medium supplemented with bovine pituitary extract (BPE) and human recombinant epidermal growth factor (EGF). All these cells were purchased from the German Resource Centre for Biological Materials (DSMZ). Cells were maintained at 37 °C in an atmosphere of 5% carbon dioxide and 95% air and underwent passage twice a week.

Cells were placed in 96-well plates at a density of 1,000 cells per well. After 24 h, plates were incubated with the amine-functionalized MSNs or an equivalent amount of free polyamine at different concentrations at 37 °C for 24 h. After removing the solution that contained the MSNs, the MTT solution (200 mL, 1 mg/mL) was added and cells were incubated for another 3 h. When the MTT solution was removed, the purple formazan crystals were solubilized with DMSO (200 mL) and measured at 560 nm on a microplate reader (SPECTRAmax plus, Molecular Devices, Sunnyvale, CA, USA). Cytotoxicity was expressed as the percentage of cell viability.

2.10. Antimicrobial effect on a real food system

The developed **N3-N** nanoparticles were used to eliminate *L. monocytogenes* from apple nectar, which was purchased in a local supermarket. The particle stock suspension was prepared in sterile distilled water and was sonicated in 3 5-minute cycles to preclude agglomerates. Different particle suspension volumes were added to 30 mL of pasteurized apple nectar. Positive and negative controls were included in the assays. Samples were inoculated with 100 μL of washed inoculum and

incubated under orbital stirring (150 rpm) at 37 ºC. After 2 h of incubation, viable cell numbers were determined as $\log_{10}$ CFU/ml by the spread plate technique using selective media and incubated at 37 °C for 48 h.

2.11. Statistical analysis

Data were statistically processed using Statgraphics Centurion XVI (Statpoint Technologies, Inc., Warrenton, VA, USA). The influence of different MSNs on bacterial viability was analyzed by an analysis of variance (one-way ANOVA). The LSD procedure (least significant difference) was used to test for any differences between averages at the 5% significance level.

3. Results and discussion

3.1. Material characterization

Silica mesoporous nanoparticles were synthesized using *N*-cetyltrimethylammonium bromide (CTABr) as a template and tetraethylorthosilicate (TEOS) as a hydrolytic inorganic precursor.[13] The solid was then calcined at 550 ºC to obtain bare MSNs (**B-N**), which were further functionalized with either *N*-(3-trimethoxysilylpropyl)diethylenetriamine (N3) or *N*-[3-(trimethoxysilyl)propyl]ethylenediamine triacetic acid trisodium salt (C3), to include nanoparticles' positive and negative charges on the surface, respectively. This resulted in amine-functionalized (**N3-N**) and carboxylate-functionalized (**C3-N**) nanoparticles.[17]

The morphology and structure of the silica mesoporous support were confirmed by field emission scanning electron microscopy (FESEM) and transmission electron microscopy (TEM). MSNs are porous nanospheres with a single-particle size of ca. 100 nm and channels of 2-3 nm which can be seen as alternate black and white stripes or as a pseudo hexagonal array of pore voids in TEM images (see Fig. 1A-B). The size distribution (Fig. 1C) and zeta potential (Fig. 1D) of bare and

functionalized nanoparticles were determined in Ringer buffer (RB). Particle size fell within the 100-220 nm range for **B-N**, whereas the zeta potential was −23.5 mV. Particle size slightly decreased after functionalization, which was most likely due to the increased colloidal stability of the nanoparticles as a result of functionalization with charged groups, which resulted in zeta potential values of -44 mV and +43 mV for **C3-N** and **N3-N**, respectively.

The degree of functionalization of solids **N3-N** and **C3-N** was determined by thermogravimetric analyses. The amount of N3 anchored to MSNs was ca. 0.36 g/g solid, while the amount of anchored C3 was ca. 0.26 g/g solid. The larger quantity of polyamines than carboxylates might be related with the fact that C3 is a bulkier molecule than N3.[17]

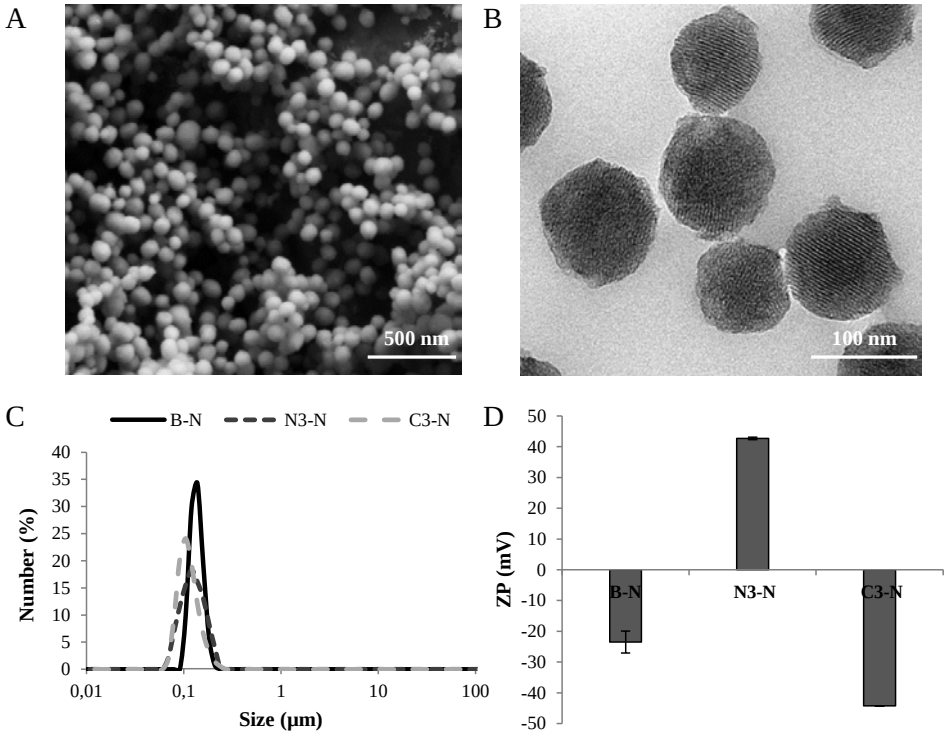

Figure 1. Material characterization of bare and functionalized MCM-41 nanoparticles. FESEM (A) and TEM (B) images of bare nanoparticles. The size distribution (C) and zeta potential (D) of bare and functionalized MSNs dispersed in RB.

3.2. Inhibitory activity of amine-functionalized nanoparticles

The use of polyamines as antimicrobial agents has been widely reported. The most important antimicrobials are the quaternary ammonium compounds with N-alkyl chain. The antimicrobial activity of these compounds involves an association between the positively charged quaternary nitrogen and the negatively charged head groups of acidic phospholipids in bacterial membranes which produces disruption of membrane integrity and leakage of cellular content.[20] They are commonly used as sanitizers in the food industry, but some toxicological issues and microbial resistances have been reported.[21-22]

Otherwise, primary and secondary amines are not considered effective antimicrobial agents. In this study, we assessed the antimicrobial activity of a primary amine immobilized onto the surface of mesoporous silica nanoparticles. The antibacterial effect of amine-functionalized nanoparticles (**N3-N**) was tested by *in vitro* viability assays of bacterial suspensions of *L. monocytogenes*. In parallel, the antimicrobial activity of **B-N**, **C3-N** and free polyamine diethylenetriamine was also evaluated. Figure 2A displays the survival of *L. monocytogenes* after 2 h of treatment when these nanoparticles were used within the 0-150 μg/mL concentration range. The results showed that **B-N** and **C3-N** had no effect on bacteria. In contrast, **N3-N** completely inhibited microbial growth at a minimum bactericidal concentration (MBC) within the 10-50 μg/mL range. The effect of free diethylenetriamine was also studied. Microbial growth was totally inhibited at a concentration as high as 2 mg/mL. In order to compare the antibacterial effect of amines alone and when attached to MSNs, Figure 2B shows the survival of *L. monocytogenes* according to the polyamine concentration for free diethylenetriamine and solid **N3-N**. As it can be observed, **N3-N** was approximately 100 times more effective as an antibacterial agent than the free polyamine against *L. monocytogenes*.

This remarkable antibacterial efficacy was most likely due to an "enhanced concentration effect" operative in **N3-N**, which boosted attractive electrostatic forces between the negatively charged bacteria and positively charged particles functionalized with amines.[23-24] Given the high local concentration of amines in nanoparticles, the interaction of the functionalized nanoparticles with the bacterial membrane of the cells was probably most effective, and resulted in improved cell structure damage (*vide infra*).

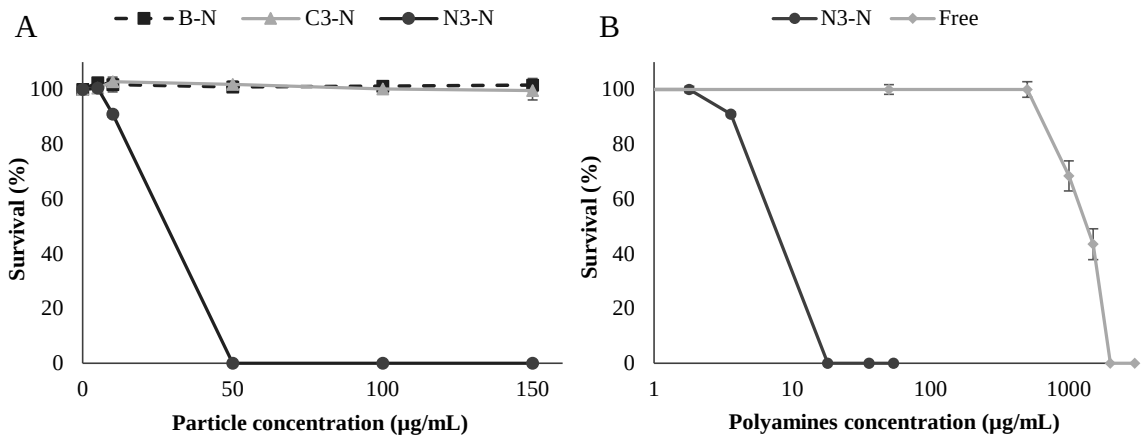

Figure 2. *L. monocytogenes* survival after incubation with bare and functionalized nanoparticles according to nanoparticle concentration (A) and *L. monocytogenes* survival after incubation with free polyamine diethylenetriamine and **N3-N** according to polyamine concentration (B) (means and standard deviations, n = 3).

3.3. Morphological changes in L. monocytogenes treated with bare and functionalized nanoparticles

In order to assess the hypothesis of the concentration effect of **N3-N** on *L. monocytogenes*, the morphological changes of this bacterium in the presence of bare and functionalized MSNs were studied by TEM. The bacteria treated with **B-N** showed the typical rod-shaped morphology of a bacterium with a complete cytoplasm and inner material surrounded by an intact cell membrane and cell wall (Fig. 3A-B). These results agree with the bacterial viability results (see Fig. 2) and with previous studies.[12-13,15,19] The cells treated with nanoparticles functionalized with carboxylates (**C3-N)** are shown in Fig. 3C-D, where both the bacterial cell wall and cell membrane appeared complete, but with roughness on some surface areas. Moreover, empty regions were observed in the cytoplasm, which could be produced by the aggregation or precipitation of internal cell components. Despite these morphological changes, bacterial viability was not affected by presence of **C3-N** (see Fig. 2), which indicates that bacteria might be able to repair this sub-lethal cell damage and maintain their viability. Finally, the TEM images of the cells treated with nanoparticles functionalized with amines (**N3-N)** are seen in Figure 3E-F. Here, bacteria cells showed severe damage, disruption of cell envelope integrity and leakage of cellular contents. These observations clearly agree with the above-described bacterial inhibition (see Fig. 2) and with the fluorescence microscopy results (*vide infra*).

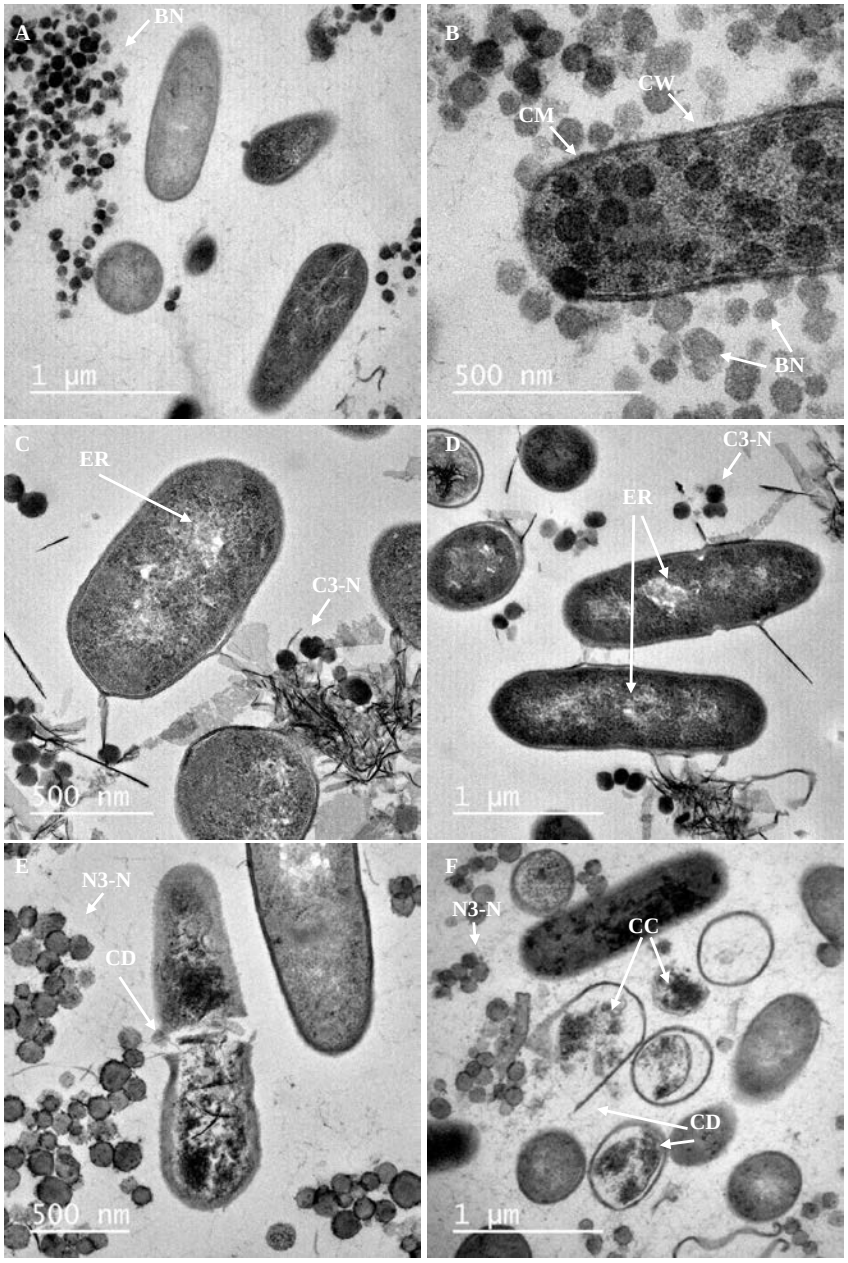

304

305 **Figure 3.** TEM micrographs by the ultrathin sectioning of *L. monocytogenes*. Images A and B
306 represent cells in the presence of bare nanoparticles; images C and D show cells treated with C3-
307 functionalized nanoparticles; and images E and F show cells in the presence of N3-functionalized
308 nanoparticles. BN: bare MCM-41nanoparticules; CW: cell wall; CM: cell membrane; ER: empty
309 regions; C3-N: carboxylate-functionalized nanoparticles; N3-N: amine-functionalized
310 nanoparticles; CC: cytoplasmic content; CD: cell wall and membrane damage.

3.4. Bacterial viability and agglomeration evaluation

Besides TEM assays, studies conducted with a two-color fluorescent LIVE/DEAD® BacLightTM assay visualized viable and dead *L. monocytogenes* cells in the presence and absence of **N3-N** nanoparticles. Figure 4A shows bacteria in the absence of **N3-N**. All the *L. monocytogenes* bacteria are green-colored, which implies that cells were viable and membranes remained intact. Figure 4B shows bacteria in the presence of **N3-N**. When **N3-N** nanoparticles were in suspension, cell aggregation was evident, and was most likely favored by the presence of positively charged nanoparticles. Red-colored cells were scattered among green cells, which indicates cell damage, and eventually bacterial death.[19] Mechanism of action could be attributed to the polyamines corona. The Gram-positive *L. monocytogenes* cell surface possesses a net negative electrostatic charge by virtue of the ionized phosphoryl and carboxylate substituent on outer cell envelope macromolecules, which are exposed to the extracellular environment.[25] In contrast, amine-functionalized MSNs possess a positive zeta potential (see Fig. 1D). Therefore, the bacterium-particle interaction driven by attractive electrostatic interactions is expected to occur.[23-24,26] This binding between the bacterial cell wall and the amine-functionalized MSNs allowed the local concentration of amines on the bacterial surface to increase, and consequently the disruption of the cell membrane, and eventually bacterial cell death.[14-15]

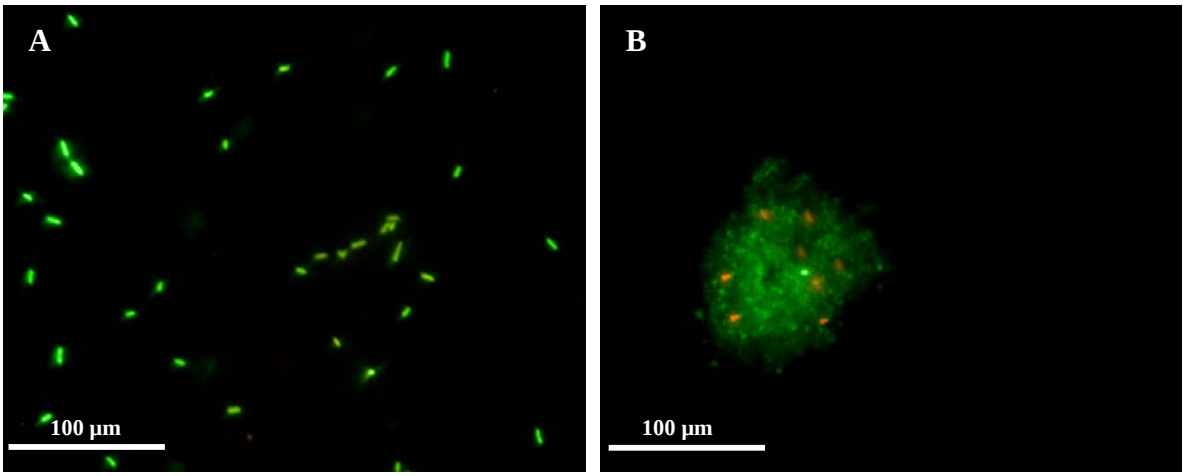

Figure 4. Fluorescence images of the untreated *L. monocytogenes* (A) and the cells treated after 2 h of incubation with **N3-N** (B). The study was performed by the two-color fluorescent LIVE/DEAD® BacLightTM assay, used to visualize viable (green) and dead (red) bacteria.

3.5. In vitro biocompatibility tests

Once the antimicrobial activity of the amine-functionalized MSNs was established, the biocompatibility of the **N3-N** solid and free polyamine to human cells was tested by WST-1 tests. As seen in Figure 5, no significant cytotoxicity of the **N3-N** nanoparticles, or an equivalent amount of free polyamine to human colon carcinoma cells (HCT116), human liver carcinoma cells (HEPG2), human kidney epithelial cells (HK2) and human cervix carcinoma cells (HeLa) cells, even at concentration as high as 150 µg/mL, was observed.

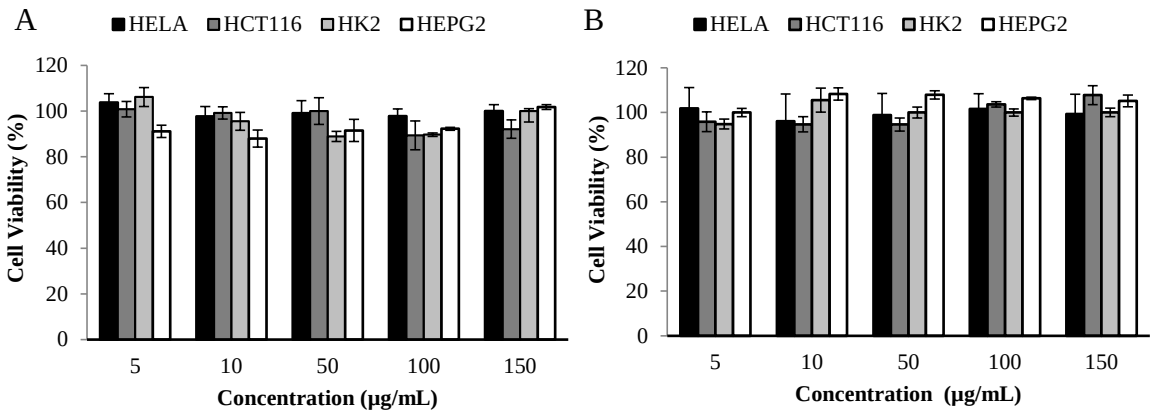

Figure 5. WST-1 cell viability assay. HeLa (black), HCT116 (dark grey), HK2 (light grey), and HEPG2 (white) cells treated with amine-functionalized nanoparticles **N3-N** (A) and the equivalent amount of free polyamine (B).

3.6. Antimicrobial activity of amine-functionalized nanoparticles in a real food system

Listeria monocytogenes is one of the most important food-borne pathogens, being responsible of a serious infection called listeriosis.[27] This bacterium is widely distributed in the environment and is generally associated with dairy products and juices, meat products, smoked fish and raw fruits and vegetables.[28] It can survive and grow over a wide range of environmental conditions such as refrigeration temperatures, low pH and high salt concentration.[29]

Microbial populations in apple juice can be inactivated by heat treatment such as pasteurization, however, potential concerns with alteration in composition and flavor properties of thermally processed fruit juices exist.[30-31] Moreover, commonly used preservatives such as potassium sorbate and sodium benzoate could be genotoxic and produce allergy problems.[32] Therefore, new technologies to prevent the spoilage and guarantee the safety of food products are needed.

The bactericidal ability of the amine-functionalized nanoparticles towards *L. monocytogenes* in a real food system (apple nectar) was investigated. The microbial growth results after 2 h of

incubation in the presence of **N3-N** are shown in Figure 6. The **N3-N** concentrations within the 1-4 mg/mL range had a clearly antibacterial effect for *L. monocytogenes*, and resulted in a remarkable complete bacteria inhibition at the **N3-N** concentration of 4 mg/mL.

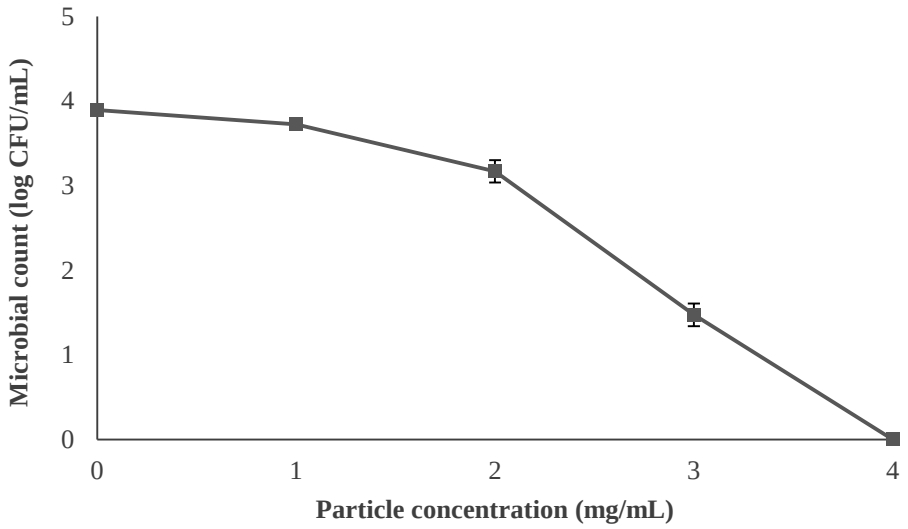

Figure 6. *L. monocytogenes* count in apple nectar after incubation with **N3-N** according to particle concentration (means and standard deviations, n = 3).

4. Conclusions

Functionalization of MSNs with amines enabled us to obtain nanodevices with 100 fold greater antimicrobial activity against *L. monocytogenes* than the equivalent quantity of free polyamine.The nanovice not only demonstrated its antibacterial activity in saline solution, but also in a food matrix. Moreover, functionalized nanoparticles were not toxic to human cells. Through microscopy images, it was demonstrated that the mechanism of action is likely due to the combination of attractive binding forces between the positive amine corona on the surface of nanoparticles and the negatively charged bacteria membrane, which provokes a disruption of cell membrane. These findings suggest

that amine-immobilized nanoparticles can be used as new antimicrobial nanodevices for diverse applications. Beyond, our study also suggests that MSN's surface functionalization opens the door to the development of new antimicrobial agents based on organic-inorganic hybrid nanosystems.

Acknowledgment

Authors gratefully acknowledge the financial support from the Ministerio de Economía y Competitividad and FEDER-EU (Projects AGL2015-70235-C2-1-R, AGL2015-70235-C2-2-R and MAT2015-64139-C4-1-R (MINECO/FEDER)). M.R.R. is grateful to the Ministerio de Educación, Cultura y Deporte for her grant (AP2010-4369). The authors also thank the Electron Microscopy Service at the UPV for support.

References

1 Capeletti LB, de Oliveira LF, Gonçalves KDA, de Oliveira JF, Saito Â, Kobarg J, Cardoso MB. Tailored silica–antibiotic nanoparticles: overcoming bacterial resistance with low cytotoxicity. *Langmuir **30***: 7456−7464 (2014).

2 Al Shamsi M, Al Samri MT, Al-Salam S, Conca W, Shaban S, Benedict S, Tariq S, Biradar AV, Penefsky HS, Asefa T, Souid AK. Biocompatibility of calcined mesoporous silica particles with cellular bioenergetics in murine tissues. *Chem Res Toxicol* **23**: 1796−1805 (2010).

3 Aznar E, Oroval M, Pascual L, Murguía JR, Martínez-Máñez R, Sancenón F. Gated materials for on-command release of guest molecules. *Chem Rev* **116**: 561−718 (2016).

4 Botequim D, Maia J, Lino MMF, Lopes LMF, Simoes PN, Ilharco LM, Ferreira L. Nanoparticles and surfaces presenting antifungal, antibacterial and antiviral properties. *Langmuir* **28**: 7646−7656 *(*2012).

5 Pérez-Esteve É, Ruiz-Rico M, Martínez-Máñez R, Barat JM. Mesoporous Silica-Based Supports for the Controlled and Targeted Release of Bioactive Molecules in the Gastrointestinal Tract. *J Food Sci* **80**:E2504-E2516 (2015).

6 Slowing II, Vivero-Escoto JL, Wu CW, Lin VSY. Mesoporous silica nanoparticles as controlled release drug delivery and gene transfection carriers. *Adv Drug Deliv Rev 60:*1278−1288 (2008)

7 Tang F, Li L, Chen D. Mesoporous silica nanoparticles: synthesis, biocompatibility and drug delivery. *Adv Mater **24***: 1504−1534 (2012).

8 Zhao Y, Sun X, Zhang G, Trewyn BG, Slowing II, Lin VSY. Interaction of mesoporous silica nanoparticles with human red blood cell membranes: size and surface effects. *ACS nano* **5**: 1366−1375 (2011).

9 Molina-Manso D, Manzano M, Doadrio JC, Del Prado G, Ortiz-Pérez A, Vallet-Regí M, Gómez-Barrena E, Esteban J. Usefulness of SBA-15 mesoporous ceramics as a delivery system for

vancomycin, rifampicin and linezolid: a preliminary report. *Int J Antimicrob Ag* **40**: 252–256 (2012).

10 Park SY, Barton M, Pendleton P. Controlled release of allyl isothiocyanate for bacteria growth management. *Food Control **23***: 478–484 (2012).

11 Bernardos A, Marina T, Žáček P, Pérez-Esteve E. Antifungal effect of essential oil components against *Aspergillus niger* when loaded into silica mesoporous supports. *J Sci Food Agr **95**:* 2824–2831 (2014).

12 Yu E, Galiana I, Martínez-Máñez R, Stroeve P, Marcos MD, Aznar E, Sancenón F, Murguía JR, Amorós P. Poly (N-isopropylacrylamide)-gated Fe_3O_4/SiO_2 core shell nanoparticles with expanded mesoporous structures for the temperature triggered release of lysozyme. Colloids Surf B **135**: 652–660 (2015).

13 Ruiz-Rico M, Fuentes C, Pérez-Esteve E, Jiménez-Belenguer AI, Quiles A, Marcos MD, Martínez-Máñez R, Barat JM. Bactericidal activity of caprylic acid entrapped in mesoporous silica nanoparticles. *Food Control* **56**: 77–85 (2015).

14 Li LL, Wang H. Enzyme-coated mesoporous silica nanoparticles as efficient antibacterial agents *in vivo*. *Adv Health Mater* **2**: 1351–1360 (2013).

15 Qi G, Li L, Yu F, Wang H. Vancomycin-modified mesoporous silica nanoparticles for selective recognition and killing of pathogenic gram-positive bacteria over macrophage-like cells. *ACS Appl Mater Interfaces* **5**: 10874–10881 (2013).

16 Mas N, Galiana I, Mondragón L, Aznar E, Climent E, Cabedo N, Sancenón F, Murguía JR, Martínez-Máñez R, Marcos MD, Amorós P. Enhanced efficacy and broadening of antibacterial action of drugs via the use of capped mesoporous nanoparticles. *Chem Eur J* **19**: 11167–11171 (2013).

17 Pérez-Esteve E, Oliver L, García L, Nieuwland M, de Jongh HH, Martínez-Máñez R, Barat JM. Incorporation of mesoporous silica particles in gelatine gels: effect of particle type and surface modification on physical properties. *Langmuir* **30**: 6970–6979 (2014).

18 Ortuño C, Quiles A, Benedito J. Inactivation kinetics and cell morphology of *E. coli* and *S. cerevisiae* treated with ultrasound-assisted supercritical CO_2. *Food Res Int* **62***:* 955-964 (2014).

19 Wehling J, Volkmann E, Grieb T, Rosenauer A, Maas M, Treccani L, Rezwan K. A critical study: Assessment of the effect of silica particles from 15 to 500 nm on bacterial viability. *Environ Pollut* **176**, 292–299 (2013).

20 Buffet-Bataillon S, Tattevin P, Bonnaure-Mallet M, Jolivet-Gougeon A. Emergence of resistance to antibacterial agents: the role of quaternary ammonium compounds-a critical review. *Int J Antimicrob Agents* **39***:* 381–389 (2012).

21 Aase B, Sundheim G, Langsrud S, Rørvik LM. Occurrence of and a possible mechanism for resistance to a quaternary ammonium compound in *Listeria monocytogenes*. *Int J Food Microbiol* **62**: 57–63 (2000).

22 Thorsteinsson T, Másson M, Kristinsson KG, Hjálmarsdóttir MA, Hilmarsson H, Loftsson T. Soft antimicrobial agents: synthesis and activity of labile environmentally friendly long chain quaternary ammonium compounds. *J Med Chem* **46**: 4173–4181 (2003).

23 Huang YF, Wang YF, Yan XP. Amine-functionalized magnetic nanoparticles for rapid capture and removal of bacterial pathogens. *Environ Sci Technol* **44**: 7908–7913 (2010).

24 Zhan S, Yang Y, Shen Z, Shan J, Li Y, Yang S, Zhu D. Efficient removal of pathogenic bacteria and viruses by multifunctional amine-modified magnetic nanoparticles. *J Hazard Mater* **274***:* 115–123 (2014).

25 Hajipour MJ, Fromm KM, Ashkarran AA, de Aberasturi DJ, de Larramendi IR, Rojo T, Serpooshan V, Parak WJ, Mahmoudi M. Antibacterial properties of nanoparticles. *Trends Biotechnol* **30**:4 99–511 (2014).

462 26 Singh S, Barick KC, Bahadur D. Surface engineered magnetic nanoparticles for removal of toxic
463 metal ions and bacterial pathogens. *J Hazard Mater* **192**: 1539–1547 *(*2011)
464 27 Gandhi M, Chikindas ML. Listeria: a food-borne pathogen that knows how to survive. *Int J*
465 *Food Microbiol* **113**: 1–15 (2007).
466 28 McLauchlin J, Mitchell RT, Smerdon WJ, Jewell K. *Listeria monocytogenes* and listeriosis: a
467 review of hazard characterisation for use in microbiological risk assessment of foods. *Int J Food*
468 *Microbiol*. **92**: 15–33 (2004).
469 29 Carpentier B, Cerf O. Review-Persistence of *Listeria monocytogenes* in food industry equipment
470 and premises. *Int J Food Microbiol* **145**: 1–8 (2011).
471 30 Baskaran SA, Amalaradjou MAR, Hoagland T, Venkitanarayanan K. Inactivation of
472 *Escherichia coli* O157: H7 in apple juice and apple cider by trans-cinnamaldehyde. *Int J Food*
473 *Microbiol* **141***:* 126-129 (2010).
474 31 Palgan I, Caminiti IM, Muñoz A, Noci F, Whyte P, Morgan DJ, Cronin DA, Lyng JG.
475 Effectiveness of high intensity light pulses (HILP) treatments for the control of *Escherichia coli* and
476 *Listeria innocua* in apple juice, orange juice and milk. *Food Microbiol* **28**: 14-20 (2011).
477 32 Zengin, N, Yüzbaşıoğlu D, Ünal F, Yılmaz S, Aksoy H. The evaluation of the genotoxicity of
478 two food preservatives: sodium benzoate and potassium benzoate. *Food Chem Toxicol* **49**: 763–769
479 (2011).